Journal of Science and Engineering Technology, Vol. 3, No. 4, pp. 17-28 (2007)

Optimal Load Tracking Design for a Catalytic-Partial-Oxidation-Based Fuel Processing System

HUAN-LIANG TSAI
Department of Electrical Engineering, Da-Yeh University
No. 112, Shanjiao Rd., Dacun, Changhua, Taiwan 51591, R.O.C.

ABSTRACT

This report presents an optimal control system design for a fuel processing system (FPS) using a generalized linear quadratic Gaussian and loop transfer recovery (LQG/LTR) method. The FPS uses natural gas as fuel and works with a catalytic partial oxidation (CPO) reaction. The control objective focuses on the regulation performances of an output vector in response to a stack current command. First, an optimal controller was designed subject to a generalized linear quadratic performance index to shape the target feedback loop function. Then a Kalman filter was designed to provide an optimal estimation of state variables for minimum and non-minimum phase plants in an LTR process. The proposed method provides another degree-of-freedom in optimal controller design and enables the compensated system to maintain a prescribed degree of stability. Finally, numerical simulations reveal that the proposed method achieves better performance and robustness properties in time- and frequency-domain responses.

Key Words: generalized LQG/LTR method, catalytic partial oxidation, fuel processing system

以觸媒不完全氧化之燃料處理系統的負載追蹤最佳化設計

蔡渙良
大葉大學電機工程學系
彰化縣大村鄉山腳路 112 號

摘　要

本論文運用文中推導的通用型線性二次高斯及迴路轉移函數回歸法的設計法則，進行一個以天然氣爲燃料、觸媒不完全氧化反應之燃料處理系統的負載追蹤最佳化控制系統設計，最佳化控制法則係以燃料電池輸出的電流大小爲負載追蹤目標。控制的目標集中在調整燃料處理系統輸出向量的反應。首先要設計一個最佳控制器滿足通用型二次線性性能指標，然後設計卡門濾波器來提供一個最佳化狀態變數的估測。本文所提出的方法可以適用於極小相和非極小相的系統，同時提供一個額外的設計自由度及特定的穩定度。最後，本文以觸媒不完全氧化的天然氣燃料處理系統爲例，經由數值模擬分析，顯示本方法在時域和頻域響應有較好的性能和穩定性特性。

關鍵詞：通用型線性二次高斯及迴路轉移函數回歸法，觸媒不完全氧化，燃料處理系統

I. INTRODUCTION

Fuel cell systems (FCSs) are publicly intended for stationary and mobile power production with low emissions and high efficiency. A typical FCS consists of fuel processing system (FPS), fuel cell stack, and power condition unit. FPS can convert fossil and/or renewable fuel soureces into suitable fuels, especially hydrogen production, for follow-up fuel cell applications. Among all primary fossil fuels, natural gas is the cleanest and the most environment-friendly fuel resource in terms of its products of combustion. Although it is a non-renewable fuel resource, natural gas is naturally preferred as the first candidate of available fuels because of its wide availability [5], high-efficient hydrogen reforming [1, 3], environmental friendliness, and sufficient infrastructure for refueling, distribution, and storage. Thus, natural gas will play an important role in the ever-increasing electric power systems in the coming future. Common methods of hydrogen reforming are pure steaming reforming (SR), catalytic partial oxidation (CPO), and autothermal reforming (ATR) with a mixture of above two methods. On one hand, SR process of natural gas produces high concentration of hydrogen generation. Suffering from poor transient operation, this reforming process is adequate for stationary operation of residential and commercial power system. On the other hand, both CPO and ATR processes of natural gas are suitable for mobile applications with rapid start-up, good tracking ability of load variation, and compactness. Nevertheless, CPO reactor suffers from the lowest hydrogen concentration and reforming efficiency than the steam reforming [3]. ATR process is the most efficient technique in all of the hydrogen reforming ones. Yet, it also achieves lower concentration of hydrogen yield than one of SR method.

In this paper a natural gas FPS with a CPO reformer for mobile applications was considered. The chemical composition of natural gas varies according to the source and its principal component in the high-pressure pipeline or tank is usually methane (CH_4). Most of hydrogen is generated in the CPO reformer where methane reacts with oxygen through a high-temperature catalytic bed. The temperature of fixed-bed catalyst and the oxygen to carbon ratio of air and fuel primarily affect the conversion efficiency of hydrogen reforming and the hydrogen concentration of hydrogen-rich synthesis gas [16, 26]. In order to accommodate the load changes in a fuel cell stack, the mole flow rate of hydrogen should be adapted to meet the power requirements with a stable temperature in CPO reactor and provide a smooth molar fraction of hydrogen in the anode of proton exchange membrane fuel cell (PEMFC) system. Pukrushpan et al. [13-15] have used a well-developed linear Quadratic (LQ) optimization technique to design an observer-based state-feedback controller for a CPO-based natural gas FPS. In fact, it is much reasonable to treat the required stack current in face of load variation as reference comand input, especially in an optimal observer design using the Kalman filter method. In addition, the controlled CPO-based FPS is non-minimum phase. The objectives of CPO-based FPS control system are usually focused on the performance and stability specifications, such as reference command tracking, disturbance rejection, and robustness characteristics. Such requirements can be naturally transformed into frequency-domain requirements in term of the singular values of sensitivity function and complementary sensitivity function in a closed-loop compensated system. The sensitivity function is related to the return ratio which is evaluated by breaking at either the input or output point of compensated plant. On the other hand, a Linear Quadratic Gaussian and Loop Transfer Recovery (LQG/LTR) process, originally proposed by Doyle et al. [7], provides a prominent “loop shaping” concept in a two-step design procedure for the corresponding principal gains of return ratio [18]. The first step is to design an optimal state-feedback controller subject to LQ performance index and also “loop shaping” the above target loop transfer function at the plant input point to meet satisfactory specifications. In the second step, an observer is obtained by recovering the return ratio of LQG-compensated plant. These motivate us develop a Generalized LQG/LTR (GLQG/LTR) method to design an optimal control system of general plant including minimum-phase and nonminimum-phase systems [4, 20-25].

The objectives of this paper are to first propose a GLQG/LTR method and then to apply the proposed technique to an optimal control system design for a CPO-based natural gas fuel processing system with a nonminimum-phase behavior as well as to unveil the better robustness and performances properties of proposed method. The remainder of this paper is organized as follows. For easy of presentation, the dynamic equations of CPO-based fuel processing system are firstly briefed in Section II. And then we derive a generalized LQG/LTR methodology for a general system, which a state-feedback controller subject to generalized linear quadratic (GLQ) performance index is first derived to shape the target loop transfer function and then a Kalman filter is designed to provide an optimal state estimation in the LTR procedure. In section III we demonstrate an optimal control system design with the proposed method for a CPO-based fuel processing system in a nonminimum-phase form, and unveils comparisons with those controllers obtained by a traditional LQG/LTR

method. Finally, brief conclusions are drawn in Section IV.

II. PROBLEM AND METHODOLOGY FORMULATION

1. CPO-Based Natural Gas FPS Model

A simplified structure of CPO-based natural gas fuel processing system [13-15] is shown in Fig. 1. This system uses natural gas as fuel and acts on catalytic partial oxidation (CPO) reaction. In general, natural gas can be furnished to a fuel processing system through a high-pressure pipeline or tank. Natural gas cannot be removed a small amount of sulfur compounds in a high-temperature or low-temperature desulfurizer [5] depending on the scale of FPS. On the other hand, a blower draws air from atmosphere and then the air is preheated in a heat exchanger. Both heated air flow and desulfurized natural gas are then mixed together in a mixer and the mixture is then passed through a catalytic bed inside CPO reactor. It is anticipated that there are two main chemical reactions, partial oxidation (POX) and total oxidation (TOX), taking place in a CPO reactor [16, 26].

$$\mathrm{CH_4} + \frac{1}{2}\mathrm{O_2} \rightarrow \mathrm{CO} + 2\mathrm{H_2}\,, \quad \Delta H_{POX} = -0.36\times 10^5\ \mathrm{J/mole} \tag{1}$$

and

$$\mathrm{CH_4} + 2\mathrm{O_2} \rightarrow \mathrm{CO_2} + 2\mathrm{H_2O}\,, \quad \Delta H_{TOX} = -0.8026\times 10^6\ \mathrm{J/mole} \tag{2}$$

It is obvious that hydrogen production only producesd from the POX reaction; therefore, to promote POX reaction is preferable to have better hydrogen selectivity. In addition, TPO reaction emits higher enthalpy and proper fraction of TPO reaction maintains the desired temperature of CPO reactor. The difference in the ratio of two reactions can be defined as the selectivity function *S*, which strongly depends on the oxygen to carbon ratio. CO created by POX reaction poisons PEMFC system and is then eliminated by using two high-temperature and low-temperature water gas shift (WGS) reactors [6, 10-12, 19] and preferential oxidation (PROX) reactor [9, 17]. In the high-temperature (about 310-450°C) and low-temperature (about 200-250°C) WGS reactors, water is injected into the reformate stream to react with CO

$$\mathrm{CO} + \mathrm{H_2O} \rightarrow \mathrm{CO_2} + \mathrm{H_2} \tag{3}$$

Since the level of CO in the gas stream after WGS reactors is normally still high for PEMFC system, air is injected into a PROX reactor and oxygen in the air reacts with the remnant CO.

$$2\mathrm{CO} + \mathrm{O_2} \rightarrow 2\mathrm{CO_2} \tag{4}$$

The overall dynamic behaviors of FPS model are developed to describe the mass flows and pressures of individual components in the FPS and the temperature of CPO. The simplified dynamic model and the associated state variables of FPS [13-15] are shown in Fig. 2. To simplify the FPS model, it is assumed that both heat exchanger and desulfurizer are viewed as volumes where the reactions are neglected. In addition, the WGS and PROX reactors, which are mainly used for CO removal, are lumped together as a combined volume (WPO). On the other hand, the gas compositions in the mixer, WPO reactors, and PEMFC anode are described with the total pressure of all compositions and additional partial pressure of important species. The blower can be modeled in the form of first-order model with a maximum rotation rate 3600 rpm. The governing equation is

$$\dot{r}_{\mathrm{BLO}} = \frac{1}{\tau_{\mathrm{BLO}}}(36u_{\mathrm{BLO}} - r_{\mathrm{BLO}}) \tag{5}$$

where r_{BLO}, τ_{BLO}, and u_{BLO} are the rotational rate, time constant, and input command of blower, respectively. The mass flow rate $W^{\mathrm{air}}_{\mathrm{BLO}}$ of inlet air in the blower is then

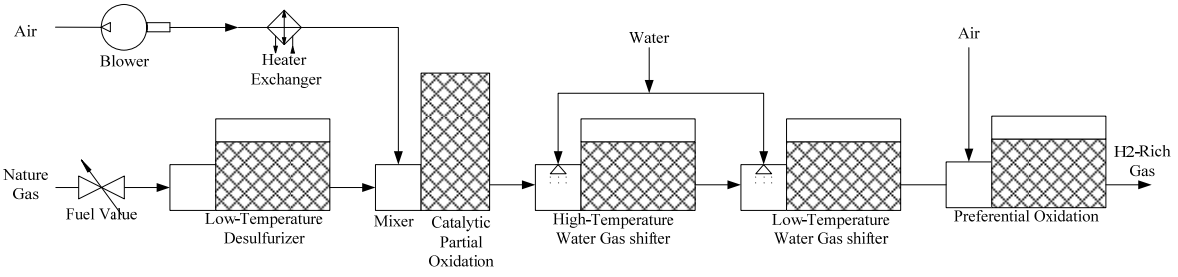

Fig. 1. Simplified Structure of CPO-Based FPS

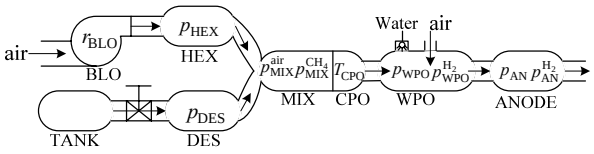

Fig. 2. Dynamic model of CPO-Based FPS

calculated by

$$W_{BLO}^{air} = r_{BLO}\rho^{air} \tag{6}$$

where ρ^{air} is the air density (=1.23kg/m^3). The mass conversation with an ideal gas law through an isothermal assumption is used to model the pressure dynamics of gas in all component volume in the fuel processing system. In general, the pressure dynamics of a species in volume of component is described by

$$\dot{p}_{VOL}^{SPE} = \frac{RT_{VOL}}{M^{SPE}V_{VOL}}(W_{VOL,in}^{SPE} - W_{VOL,out}^{SPE}) \tag{7}$$

where R is the universal gas constant, T_{VOL} and V_{VOL} are respectively the temperature and gas volume of component, M^{SPE} is the molecular weight of species, and $W_{VOL,in}^{SPE}$ and $W_{VOL,out}^{SPE}$ are the inlet and outlet mass flow rates of species in a component, respectively. With a turbulent flow assumption, the mass flow rate through an orifice can be approximately calculated from the pressure difference between upstream pressure p_{in} and downstream pressure p_{out} by using nozzle flow equation [8]

$$W = W_0\sqrt{\frac{p_{in} - p_{out}}{\Delta p_0}} \tag{8}$$

where W_0 and Δp_0 are the nominal mass flow rate of species and the nominal pressure drop of the orifice, respectively. If the pressure difference between manifold and downstream volume is small, the above sub-critical nozzle flow equation can be linearized as

$$W = k(p_{in} - p_{out}) \tag{9}$$

where k is the nozzle resistance constant. Take a heat exchanger for example,

$$\dot{p}_{HEX} = \frac{RT_{HEX}}{M^{air}V_{HEX}}(W_{BLO}^{air} - W_{HEX}^{air}) \tag{10}$$

where p_{HEX} is the pressure of heat exchanger, T_{HEX} and V_{HEX} are, respectively the temperature and volume of heat exchanger, M^{air} is the molar mass of air (=2.74×10^{-2}kg/mole), and W_{HEX} is the mass flow rate of air into the mixer, which can be approximately linearized as

$$W_{HEX} = k_{HEX}(p_{HEX} - p_{MIX}^{air}) \tag{11}$$

where k_{HEX} is the nozzle resistance of heat exchanger and p_{MIX}^{air} is the partial pressure of air in the mixer. The pressure dynamics of heat exchanger is rewritten in a linearized form

$$\dot{p}_{HEX} = \frac{RT_{HEX}}{M^{air}V_{HEX}}[\rho^{air}r_{BLO} - k_{HEX}(p_{HEX} - p_{MIX}^{air})] \tag{12}$$

The only dynamics considered in a CPO reactor is the temperature of catalyst bed and is modeled using the energy balance equation

$$\dot{T}_{CPO} = \frac{1}{m_{CPO}C_{CPO}}(H_{in} - H_{out} + \Delta H) \tag{13}$$

where m_{CPO} (kg) and C_{CPO} (J/kg·K) are the mass and heat capacity of catalyst bed, H_{in} and H_{out} are the enthalpies of inlet and outlet flows of CPO reactor, and ΔH is the heat produced by the reaction in the CPO reactor. Two performance variables, which are the H_2 molar fraction in the anode $\lambda_{AN}^{H_2}$ and CPO temperature, need to be regulated to maintain high-efficiency hydrogen utilization and conversion. The H_2 molar fraction in the anode $\gamma_{AN}^{H_2}$ can be calculated by

$$\gamma_{AN}^{H_2} = \frac{p_{AN}^{H_2}}{p_{AN}} \tag{14}$$

Therefore, a linearized model of the CPO-based FPS in [13-15] can be reformulated in the form of state-space realization.

$$\dot{x} = Ax(t) + B_u u(t) + B_r r_c(t) \tag{15}$$

and

$$y = Cx(t) \tag{16}$$

with

$$A=\begin{bmatrix} -3.333 & 0 & 0 & 0 & 0 & 0 & 0 & 0 & 0 & 0 \\ 212.63 & -124.5 & 0 & 112.69 & 112.69 & 0 & 0 & 0 & 0 & 0 \\ 0 & 0 & -32.43 & 32.304 & 32.304 & 0 & 0 & 0 & 0 & 0 \\ 0 & 221.97 & 0 & -254.9 & -253.2 & 0 & 0 & 32.526 & 0 & 0 \\ 0 & 0 & 331.8 & -341 & -344 & 0 & 0 & 0 & 0 & 0 \\ 0 & 0 & 0 & 1.0748 & -3.53 & -0.074 & 0 & 1\times10^{-6} & 0 & 0 \\ 0 & 0 & 0 & 1.214 & 1.8309 & 0 & -0.358 & -3.304 & 0 & 2.0354 \\ 0 & 0 & 0 & 5.3994 & 5.6043 & 0.0188 & 0 & -13.61 & 0 & 8.1642 \\ 0 & 0 & 0 & 0 & 0 & 0 & 2.5582 & 13.911 & -1.468 & -25.3 \\ 0 & 0 & 0 & 0 & 0 & 0 & 0 & 0 & 33.586 & -156 \end{bmatrix} \tag{17}$$

$$B_u=\begin{bmatrix} 0.12 & 0 & 0 & 0 & 0 & 0 & 0 & 0 & 0 & 0 \\ 0 & 0 & 0.1834 & 0 & 0 & 0 & 0 & 0 & 0 & 0 \end{bmatrix}^T \tag{18}$$

$$B_r=\begin{bmatrix} 0.0265 & 0 & 0.0504 & 0 & 0 & 0 & 0 & 0 & -0.328 & -0.024 \\ 1 & 0 & 0 & 0 & 0 & 0 & 0 & 0 & 0 & 0 \\ 0 & 0 & 1 & 0 & 0 & 0 & 0 & 0 & 0 & 0 \end{bmatrix}^T \tag{19}$$

and

$$C=\begin{bmatrix} 0 & 0 & 0 & 0 & 0 & 1 & 0 & 0 & 0 & 0 \\ 0 & 0 & 0 & 0 & 0 & 0 & 0 & 0 & 0.994 & -0.088 \end{bmatrix} \tag{20}$$

where the state, input, and output vectors of dynamic equations are defined as

$$x(t)=\begin{bmatrix} p_{\mathrm{BLO}} & p_{\mathrm{HEX}} & p_{\mathrm{DES}} & p_{\mathrm{MIX}}^{\mathrm{air}} & p_{\mathrm{MIX}}^{\mathrm{CH_4}} & T_{\mathrm{CPO}} & p_{\mathrm{WPO}}^{\mathrm{H_2}} & p_{\mathrm{WPO}} & p_{\mathrm{AN}}^{\mathrm{H_2}} & p_{\mathrm{AN}} \end{bmatrix}^T \tag{21}$$

$$u(t)=\begin{bmatrix} u_{\mathrm{BLO}} & u_{\mathrm{VAL}} \end{bmatrix}^T \tag{22}$$

$$r_c(t)=\begin{bmatrix} T_{\mathrm{CPO},r} & \gamma_{\mathrm{AN}}^{\mathrm{H_2}} & I_{st} \end{bmatrix}^T \tag{23}$$

and

$$y(t)=\begin{bmatrix} T_{\mathrm{CPO}} & \gamma_{\mathrm{AN}}^{\mathrm{H_2}} \end{bmatrix}^T \tag{24}$$

2. Problem Definition

Let the dynamic equations of multivariable control system shown in Fig. 3 be as follows

$$\dot{x}(t)=Ax(t)+B_u u(t)+B_r r_c(t)+\Gamma w(t) \tag{25}$$

and

$$y(t)=Cx(t)+v(t) \tag{26}$$

where $x(t)\in\Re^{\mathrm{n}}$, $u(t)\in\Re^{\mathrm{m}}$, $r_c(t)\in\Re^{\mathrm{r}}$, and $y(t)\in\Re^{\mathrm{q}}$ are the state, input, reference command, and output vectors, respectively, $A\in\Re^{\mathrm{n\times n}}$, $B_u\in\Re^{\mathrm{n\times m}}$, $B_r\in\Re^{\mathrm{n\times r}}$, $\Gamma\in\Re^{\mathrm{n\times p}}$, and $C\in\Re^{\mathrm{q\times n}}$ are the state, input of control, input of reference command, input of disturbance, and output matrices, respectively. The system disturbance $w(t)$ and the measurement noise $v(t)$ are, respectively, p- and q-dimensional uncorrelated Gaussian white noise processes with zero-mean, and the covariances are given by

$$E\{w(t)w^T(\tau)\}=W(t)\delta(t-\tau) \tag{27}$$

$$E\{v(t)v^T(\tau)\}=V(t)\delta(t-\tau) \tag{28}$$

And

$$E\{v(t)w^T(\tau)\}=0 \tag{29}$$

where $E\{\cdot\}$ is an expectation function operator, $W(t)$ and $V(t)$ are system disturbance and measurement noise covariance matrices, respectively. The nominal plant (A, B_u, C) is said to be non-minimum phase if there exists at least one transmission

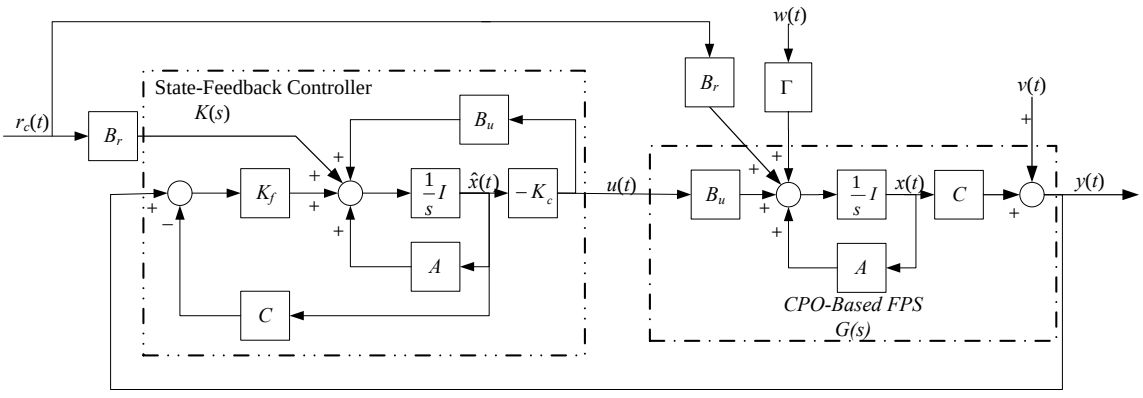

Fig. 3. GLQG/LTR control structure

zero of its transfer function $G(s)$ contained in the open right half of the complex plane, where $G(s) = C(sI - A)^{-1}B_u$.

The problem is to derive an optimal control law minimizing the following GLQ performance index

$$J = E\{\frac{1}{2}\int_0^{t_f} e^{2\sigma t}[y^T(t)Qy(t) + u^T(t)Ru(t)]dt\} \quad (30)$$

where Q is a q×q positive semi-definite weighting matrix, R is an m×m positive definite control weighting matrix, and α is a nonnegative constant which can provide a prescribed degree of stability in the proposed regulation problem.

3. Methodology Formulation

According to the separation principle, a state-feedback controller is designed subject to the GLQ performance index and is used to shape the principal gains of return ratio for a target loop gransfer function at the input of controlled plant. Secondly a Kalman filter is designed to provide an optimal estimated state vector in the LTR process.

A. Target loop transfer function at plant input

According to above GLQ performance index, the optimal control law for a state-feedback controller can be derived as follows. Firstly, the corresponding Hamilton function is defined as

$$H = \frac{1}{2}e^{2\alpha t}(x^T C^T QCx + u^T Ru) + P^T\left(Ax + B_u u + B_r r_c + \Gamma w\right) \quad (31)$$

The optimal control law can be obtained by solving the following Euler-Lagrange equations

$$\dot{x} = \partial H / \partial P = Ax + B_u u + B_r r_c + \Gamma w \quad (32)$$

$$\dot{P} = -\partial H / \partial x = -e^{2\alpha t}C^T QCx - A^T P \quad (33)$$

and

$$\partial H / \partial u = e^{2\alpha t}Ru + B_u^T P = 0 \quad (34)$$

with the transversality condition at the terminal time t_f

$$P(t_f) = Qx(t_f) \quad (35)$$

The optimal control law can be obtained as

$$u = -\exp(-2\alpha t)R^{-1}B_u^T P \quad (36)$$

Assume that $P=P_c x$. After some manipulations, we have

$$(\dot{P}_c + P_c A + A^T P_c - e^{-2\alpha t}P_c B_u R^{-1}B_u^T P_c + e^{2\alpha t}C^T QC)x = 0 \quad (37)$$

Since Eq. (37) is always true for any x, we obtain

$$\dot{P}_c + P_c A + A^T P_c - e^{-2\alpha t}P_c B_u R^{-1}B_u^T P_c + e^{2\alpha t}C^T QC = 0 \quad (38)$$

According to a sub-optimal control law, the control input can be obtained

$$u(t) = -K_c x(t) \quad (39)$$

where K_c is the optimal control gain matrix and is derived as

$$K_c = R^{-1}B_u^T P_c \quad (40)$$

and where P_c is a positive definite symmetric matrix, which is defined by the following Controller Algebraic Riccati equation (CARE)

$$P_c(A + \alpha I) + (A^T + \alpha I)P_c - P_c B_u R^{-1}B_u^T P_c + C^T QC = 0 \quad (41)$$

The parameter α can provide a prescribed degree of stability [2]. The optimal controller is designed to shape the open-loop principal gains of return ratio $G_t(s) = -K_c(sI - A)^{-1}B_u$ to meet the required specifications. $Gt(t)$ is thus called target loop transfer function. Its associated sensitivity function and complementary sensitivity function are defined as

$$S_f(s) = \left[I + K_c(sI - A)^{-1}B_u\right]^{-1} \quad (42)$$

and

$$T_f(s) = I - S_f(s) \quad (43)$$

The key points of optimal controller design are to make the principal gains of return ratio for the open-loop transfer function $-K_c(sI - A)^{-1}B_u$ meet the crossover frequencies, balance the principal gains as possible, and adjust the low-frequency behavior.

B. Kalman filter design in LTR process

The next step is to design a Kalman filter to obtain an optimal estimate $\hat{x}(t)$ of $x(t)$, which minimizes $E\left\{\left[x(t) - \hat{x}(t)\right]^T\left[x(t) - \hat{x}(t)\right]\right\}$. For a minimum-phase plant (A_m, B_m, C_m), the Kalman filter can be derived by the following state estimation equation

$$\dot{\hat{x}}(t) = A_m\hat{x}(t) + B_m u(t) + K_f\left[y(t) - C_m\hat{x}(t)\right] \quad (44)$$

where K_{mf} is the gain matrix of a Kalman filter calculated by

$$K_{mf} = P_{mf}C_m^T V^{-1} \quad (45)$$

and where P_{mf} is the covariance of $x(t) - \hat{x}(t)$ defined as

$$P_{mf} = E\left\{\left[x(t) - \hat{x}(t)\right]^T\left[x(t) - \hat{x}(t)\right]\right\} \quad (46)$$

P_{mf} can be obtained by the following Filter Algebraic Riccati Equation (FARE)

$$A_m P_{mf} + P_{mf}A_m^T + \Gamma W\Gamma^T - P_{mf}C_m^T V^{-1}C_m P_{mf} = 0 \quad (47)$$

It is well known that the right-hand plane (RHP) zeros of a non-minimum phase plant may be collected into a stable all-pass filter. The similar factorization is used to describe the RHP zeros in terms of structured uncertainty. Suppose the original plant is non-minimum phase, i.e. there is at least one zero in the RHP. Given a non-minimum phase system (A, B_u, C) with l RHP zeros, all the zeros can be factored in the form of multiplicative input uncertainty described as

$$G(s) = G_m(s)[1 + \Delta(s)] \quad (48)$$

where $\Delta(s) = -2z/(s+z)$ is a structured uncertainty, and $z = \sum_{i=1}^{l} z_i$ is the sum of all the RHP zeros. By this way the non-minimum phase system can be expressed as a minimum-phase plant (A_m, B_m, C_m) with RPH zeroes in the form of multiplicative uncertainty. Suppose that K_f and K_{mf} are the gain matrices of Kalman filter design for (A, B_u, C) and (A_m, B_m, C_m), respectively. It has been well-proofed that $K_f = K_{mf}$ [22-23]. Thus the gain matrix of Kalman filter for a general plant is given by

$$K_f = P_f C^T V^{-1} \quad (49)$$

where P_f can be obtained by the following Filter Algebraic Riccati Equation (FARE)

$$AP_f + P_f A^T + \Gamma W\Gamma^T - P_f C^T V^{-1} C P_f = 0 \quad (50)$$

Since the disturbances would couple into the system through the inputs rather than directly on the states, Γ is chosen as the input matrix B, i.e., $\Gamma = B$. The gain matrix of Kalman filter for a general system can be determined by manipulating the covariance matrices W and V.

Therefore, the closed-loop dynamic equation of compensated system can be arranged as

$$\begin{bmatrix}\dot{x}(t)\\ \dot{\hat{x}}(t)\end{bmatrix}^T = \begin{bmatrix} A & -B_u K_c \\ K_f C & A - B_u K_c - K_f C\end{bmatrix}\begin{bmatrix}x(t)\\ \hat{x}(t)\end{bmatrix} + \begin{bmatrix} B_r & \Gamma & 0 \\ B_r & 0 & K_f\end{bmatrix}\left[r_c(t) \quad w(t) \quad v(t)\right]^T \quad (51)$$

and

$$y(t) = \begin{bmatrix} C & 0\end{bmatrix}\begin{bmatrix}x(t)\\ \hat{x}(t)\end{bmatrix} + \begin{bmatrix}0 & 0 & I\end{bmatrix}\begin{bmatrix} y_d(t)\\ w(t)\\ v(t)\end{bmatrix} \quad (52)$$

Since the transfer function of an observer-based state feedback controller is

$$K(s) = -K_c(sI - A + BK_c + K_f C)^{-1}K_f \quad (53)$$

the resulting return ratio evaluated at the input of compensated plant is

$$G(s)K(s) = -C(sI - A)^{-1}BK_c(sI - A + BK_c + K_f C)^{-1}K_f \quad (54)$$

and the associated sensitivity function and complementary sensitivity function for the compensated plant are respectively as

$$S_{GK}(s) = [I + G(s)K(s)]^{-1} \quad (55)$$

and

$$T_{GK}(s) = S(s)G(s)K(s) \quad (56)$$

In the proposed GLQG/LTR approach, the weighting matrices Q and R in the performance index are tunable parameters. In addition, there is an additional parameter α that can be tuned to get better performance and robustness properties for a general system. In the LTR procedure, one solves the FARE defined as Eq. (50). We should manipulate them to recovery the principal gains of the return ratio $G(s)K(s)$ at the input of compensated plant to the previously obtained target loop transfer function $G_t(s)$ as close as possible.

III. NUMERICAL EXAMPLE AND SIMULATION RESULTS

The principal gains of return ratio $C(sI-A)^{-1}B$ for the nominal plant are shown in Fig. 4, where $\bar{\sigma}(\cdot)$ and $\underline{\sigma}(\cdot)$ are maximum and minimum principal gain function, respectively. It is obvious the plant is a type-0 system. It is necessary to augment the model by inserting integral action before each input to eliminate steady-state error. As the output vector is assumed to be directly measured, the state equation of the integrators is [13-14]

$$\begin{bmatrix} \dot{\varepsilon}_{T_{\rm CPO}} \\ \dot{\varepsilon}_{\gamma_{\rm AN}^{\rm H_2}} \end{bmatrix} = \begin{bmatrix} T_{\rm CPO}^{ref} - T_{\rm CPO} \\ \gamma_{\rm AN}^{\rm H_2,ref} - \gamma_{\rm AN}^{\rm H_2} \end{bmatrix} \tag{57}$$

The augmented plant is described by

$$\begin{bmatrix} \dot{x}(t) \\ \dot{\varepsilon}(t) \end{bmatrix} = \begin{bmatrix} A & 0 \\ -C & 0 \end{bmatrix} \begin{bmatrix} x(t) \\ \varepsilon(t) \end{bmatrix} + \begin{bmatrix} B_u \\ 0 \end{bmatrix} u(t) + \begin{bmatrix} B_r \\ [I_2 \quad 0] \end{bmatrix} r_c(t) + \begin{bmatrix} \Gamma \\ 0 \end{bmatrix} w(t) \tag{58}$$

and

$$\begin{bmatrix} y(t) \\ \varepsilon(t) \end{bmatrix} = \begin{bmatrix} C & 0 \\ 0 & I \end{bmatrix} \begin{bmatrix} x(t) \\ \varepsilon(t) \end{bmatrix} + \begin{bmatrix} I \\ 0 \end{bmatrix} v(t) \tag{59}$$

i.e.,

$$\dot{x}_a(t) = A_a x_a(t) + B_{ua} u(t) + B_{ra} r_c(t) + \Gamma_a w(t) \tag{60}$$

and

$$y_a(t) = C_a x_a(t) + I_a v(t) \tag{61}$$

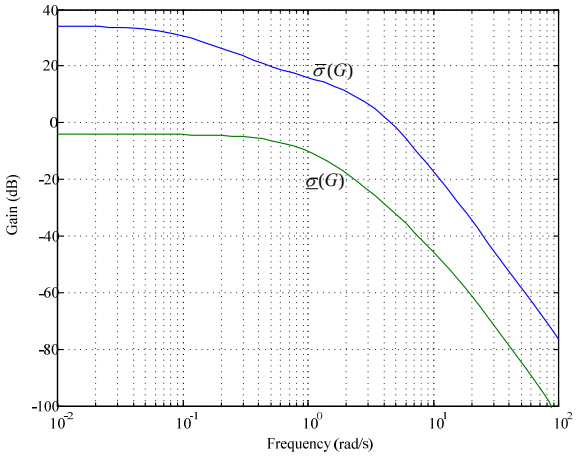

Fig. 4. Principal gains of return ratio $C(sI-A)^{-1}B$ for nominal system

with

$$x_a(t) = \begin{bmatrix} x(t) & \varepsilon(t) \end{bmatrix}^T \tag{62}$$

$$y_a(t) = \begin{bmatrix} y(t) & \varepsilon(t) \end{bmatrix}^T \tag{63}$$

The performance index is also augmented as

$$J = E\{\frac{1}{2}\int_0^{t_f} e^{2\sigma t}[x^T(t)C^T Q_y C x(t) + \varepsilon^T(t) Q_I \varepsilon(t) + u^T(t) R u(t)]dt\} \tag{64}$$

The desired output vector is selected that the operating temperature of CPO reactor is $T_{\rm CPO}$=972°K and the H_2 molar fraction in the anode is $\gamma_{\rm AN}^{\rm H_2} = 0.088$. The control objective is to regulate both $T_{\rm CPO}$=972°K and $\gamma_{\rm AN}^{\rm H_2} = 0.088$ in the reference command tracking of stack current $I_{\rm ST}$ and in face of low-frequency disturbance noise. For a mobile FCS application, a coordinated controller is designed to meet the requirements that the desired stack current $I_{\rm ST}$ is commanded to make the vehicle in the preferred maneuvering direction rapidly, and both both $T_{\rm CPO}$=972°K and $\gamma_{\rm AN}^{\rm H_2} = 0.088$ are simultaneously regulated at the required operating conditions. The desired reference command vector is defined as Eq. (23).

1. Control Design for Target Loop Transfer Function

The control input can be obtained

$$u(t) = -K_c x_a(t) \tag{65}$$

and K_c is obtained as

$$K_c = R^{-1} B_{ua}^T P_c = \begin{bmatrix} K_p & K_I \end{bmatrix} \tag{66}$$

and where P_c is a positive definite symmetric matrix, which is defined by the following Controller Algebraic Riccati equation (CARE)

$$P_c(A_a + \alpha I) + (A_a^T + \alpha I)P_c - P_c B_{ua} R^{-1} B_{ua}^T P_c + diag(C^T Q_y C, Q_I) = 0 \tag{67}$$

The weighting matrices have been chosen as Q_y=*diag*(80,1100), Q_I=*diag*(150,100), and R=*diag*(100,120) [13-14]. There is another parameter α in Eq. (67) that can be manipulated to shape the principal gains of the target loop transfer function. As $\alpha=8\times10^{-2}$, the control gain matrix is listed in Table 1. The principal gains of target loop transfer function, sensitivity function, and complementary sensitivity function at the plant input are shown in Figs. 5-6. For comparison purpose, the results obtained with a traditional LQ

Table 1. Gain matrices of Kalman filter and state-feedback controller

Kalman-Filter Gain Matrix
$K_f = \begin{bmatrix} 469.67 & 5.6245 & -93.622 & -742.29 & -30.245 & -795.89 & -2149.2 & 1400.7 & 1559.8 & -430.89 \\ 138.59 & 818.34 & -12.759 & -99.077 & -4.7928 & -104.2 & -392.69 & 294.09 & 3547.1 & -58.728 \end{bmatrix}^{\mathrm{T}}$
State-Feedback Controller Gain Matrix
$K_p = \begin{bmatrix} 1.4952 & 0.2309 & 0.0270 & 1.1284 & 41.0484 & -6.7401 & -0.7217 & 0.6393 & 0.9696 & 1.0016 \\ -0.0977 & 1.4317 & -0.1628 & -0.2545 & -8.5843 & 7.0956 & 0.7162 & -0.1446 & 4.6543 & 0.1915 \end{bmatrix}$
$K_I = \begin{bmatrix} -1.3291 & -0.2456 \\ 0.1915 & -1.3140 \end{bmatrix}$

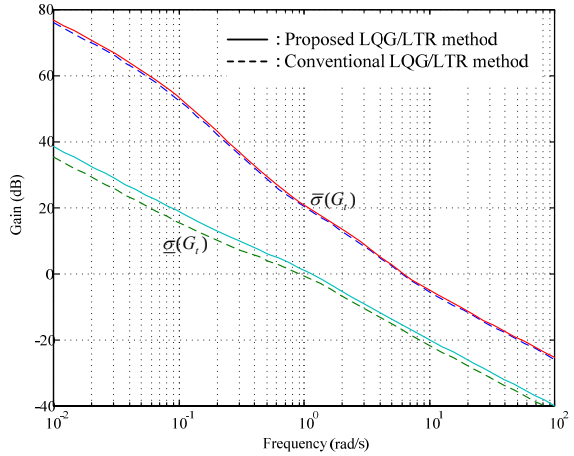

Fig. 5. Principal gains of target loop transfer function G_t(s)

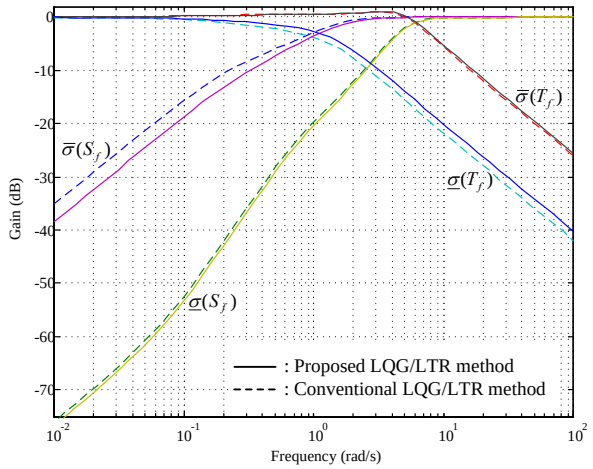

Fig. 6. Principal gains of S_f(s) and T_f(s)

method (with α=0) are also shown in Figs. 5-6. At low frequencies, the integral action is obviously visible in each channel shown in Fig. 5. In addition, Fig. 5 shows with the proposed method the maximum and minimum principal gains are increased about 2-4 dB at low frequencies and the condition number $\bar{\sigma}(G_t)/\underline{\sigma}(G_t)$ is decreased at all interested frequencies. The principal gains of sensitivity function at low frequencies are also declined about 6dB as shown in Fig. 6. These contributions make the compensated system more robust in the face of noises. The decrease of condition number $\bar{\sigma}(GK)/\underline{\sigma}(GK)$ unveil that the proposed method is much robust in face of plant's uncertainty.

2. Kalman Filter Design in LTR Process

The parameters W and V are manipulated to shape the principal gains of return ratio, sensitivity function, and complementary sensitivity function to make better recoverable quality in the LTR process. The gain matrix of Kalman filter is also listed Table 1. It should be noted that there is a tradeoff between the recoverable quality of LTR and the performance of time-domain response. The closed-loop dynamic equation of compensated system can be arranged as

$$\begin{bmatrix} \dot{x}(t) \\ \dot{\varepsilon}(t) \\ \dot{\hat{x}}(t) \end{bmatrix} = \begin{bmatrix} A & -B_u K_p & -B_u K_I \\ -C & 0 & 0 \\ K_f C & -B_u K_I & A - B_u K_p - K_f C \end{bmatrix} \begin{bmatrix} x(t) \\ \varepsilon(t) \\ \hat{x}(t) \end{bmatrix} + \begin{bmatrix} B_r & \Gamma & 0 \\ \begin{bmatrix} I_2 & 0 \end{bmatrix} & 0 & 0 \\ B_r & 0 & 0 \end{bmatrix} \begin{bmatrix} r_c(t) \\ w(t) \\ v(t) \end{bmatrix} \tag{68}$$

and

$$y(t) = \begin{bmatrix} C & 0 \end{bmatrix} \begin{bmatrix} x(t) \\ \hat{x}(t) \end{bmatrix} + \begin{bmatrix} 0 & 0 & I \end{bmatrix} \begin{bmatrix} y_d(t) \\ w(t) \\ v(t) \end{bmatrix} \tag{69}$$

The principal gains of the return ratio $G(s)K(s)$, sensitivity function $S_{GK}(s)$, and complementary sensitivity function $T_{GK}(s)$ of compensated system are shown in Figs. 7-8. For comparison purpose, the results obtained with a traditional LQG/LTR method (with α=0) are also shown in Figs. 7-8. Fig. 7 shows with the proposed method the maximum and minimum principal gains are increased about 2-4 dB at low frequencies and the condition number $\bar{\sigma}(GK)/\underline{\sigma}(GK)$ is also decreased at all interested frequencies. The principal gains of sensitivity

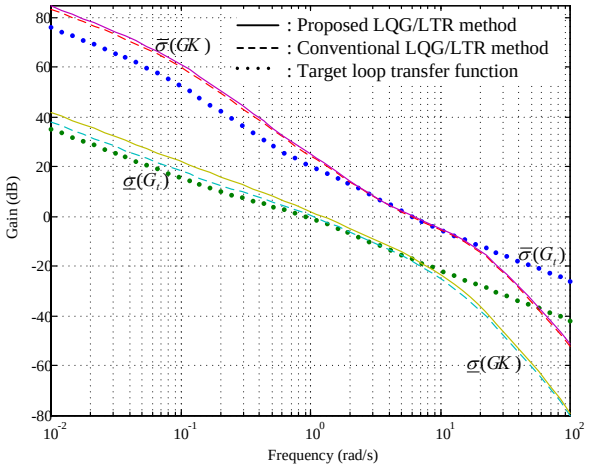

Fig. 7. Principal gains of return ratio $G(s)K(s)$ for compensated systems

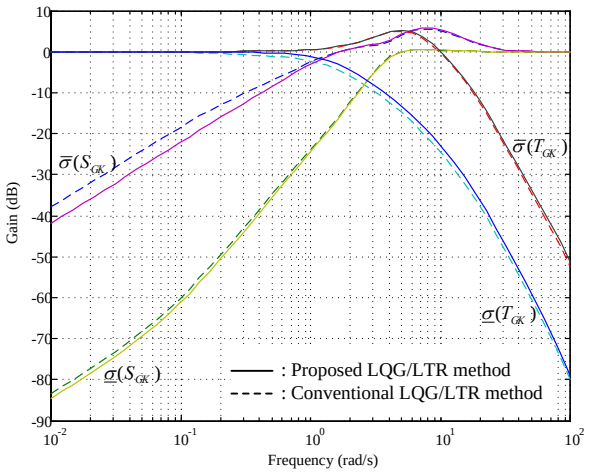

Fig. 8. Principal gains of $S_{GK}(s)$ and $T_{GK}(s)$ for compensated systems

function at low frequencies are also declined about 6dB as shown in Fig. 8. The principal gains of complementary sensitivity function at high frequencies shown in Figs. 6 and 8 demonstrate that the introduction of Kalman filter makes the compensated system increase –30 dB/decade attenuation capability. These contributions make the compensated system more robust in the presence of low-frequency and high-frequency noises. Furthermore, the time-domain simulations of compensated system in response to additional 50A command of stack current for both proposed GLQG/LTR and traditional LQG/LTR methods are simultaneously shown in Figs. 9-13. Figs. 10 and 11 unveil the proposed method has better regulation ability of CPO reactor temperature and H_2 molar fraction. In addition, the proposed method reduces the maximum input amplitudes of the blower and fuel value inputs

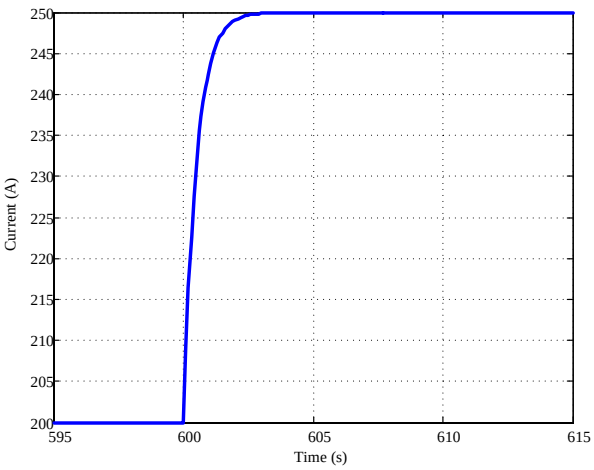

Fig. 9. Desired stack current increases by 50A in the face of load variation

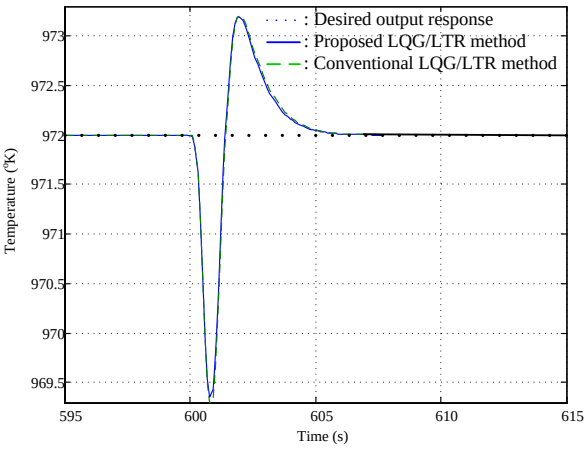

Fig. 10. Temperature response of CPO reactor for commanded stack current

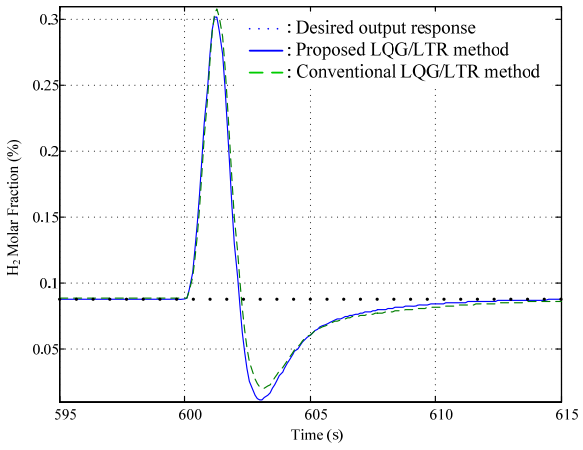

Fig. 11. H_2 molar fraction response of anode for commanded stack current

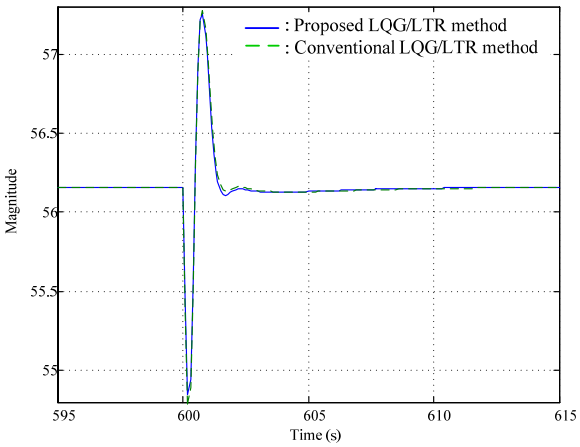

Fig. 12. Blower control input for commanded stack current

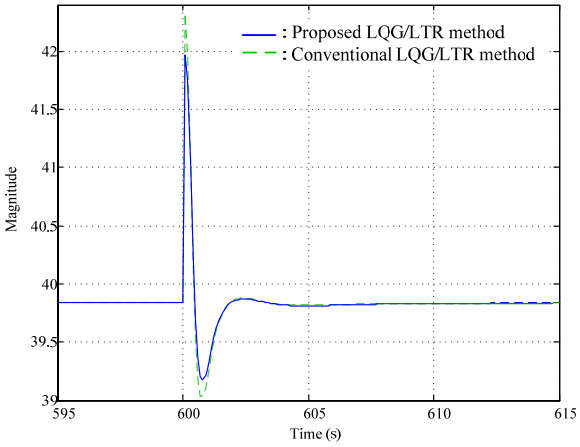

Fig. 13. Fuel value input for commanded stack current.

as shown in Figs. 12 and 13, respectively. The root mean square of both blower and fuel value inputs are also listed in Table 2. These contributions can save the power consumption of fuel processing system and improve the conversion efficiency of overall system. To evaluate the robustness of compensated system, the covariance responses of output vectors in the face of system disturbance covariance W=1 and measurement noise covariance V=1 are listed in Table 3. The proposed GLQG/LTR method lessens the deviation of operating conditions and increase the robustness and performance properties of compensated system.

IV. CONCLUSIONS

From the previous derivation and numerical simulations, the proposed GLQG/LTR method could generalize the traditional LQG/LTR technique and this makes the GLQG/LTR technique more useful in some practical applications. In addition, the introduction of tunable parameter α provides an additional degree-of-freedom of design and a prescribed degree of stability. By numerical simulations and comparisons with the results obtained by the LQG/LTR approach, the proposed method could achieve better robustness and performance properties in both frequency-domain and time-domain responses.

Table 2. Root mean square of input vector

Items	GLQG/LTR	LQG/LTR
$\mathrm{rms}(u_{\mathrm{BLO}})$	59.2979	59.2984
$\mathrm{rms}(u_{\mathrm{VAL}})$	39.9375	39.9377

Table 3. Covariances of output responses in the face of white noises

Items	GLQG/LTR	LQG/LTR
$E(e_{T_{\mathrm{CPO}}} e_{T_{\mathrm{CPO}}}^T)$	114.1195	115.8910
$E(e_{\gamma_{\mathrm{AN}}^{\mathrm{H_2}}} e_{\gamma_{\mathrm{AN}}^{\mathrm{H_2}}}^T)$	5.7413	6.4107

ACKNOWLEDGEMENTS

This research is sponsored by the project NSC 95-2212-E-212-044 from National Science Council of the Republic of China.

REFERENCES

1. Ahmed, S. and M. Krumpelt (2001) Hydrogen from hydrocarbon fuels for fuel cells. *International Journal Hydrogen Energy*, 26(4), 291-301.
2. Anderson, B. D. O. and J. B. Moore (1990) *Optimal Control: Linear Quadratic Methods*, 60-67, 207-261. Prentice-Hall International, New Jersey, NJ.
3. Brown, L. F. (2001) A comparative study of fuels for on-board hydrogen production for fuel-cell-powered automobiles. *International Journal Hydrogen Energy*, 26(4), 381-397.
4. Chang H. S. and H. L. Tsai (2006) General LQG/LTR control of catalytic-partial-oxidation-based fuel processing system. Proceedings of 2006 CACS Automatic Control Conference, Tamsui, Taiwan.
5. Dicks, A. L. (1996) Hydrogen generation from natural gas for the fuel cell systems of tomorrow. *Journal of Power Sources*, 61(1-2), 113-124.
6. Doss, E. D., R. Kumar, R. K. Ahluwalia and M. Krumpelt (2001) Fuel processors for automotive fuel cell systems: A parametric analysis. *Journal of Power Sources*, 102(1-2), 1-15.
7. Doyle, J. C. and G. Stein (1981) Multivariable feedback

design: Concepts for a classical / modern synthesis. *IEEE Transaction on Automatic Control*, AC-26(1), 4-16.

8. Heywood, J. B. (1988) *Internal Combustion Engine Fundamentals*, 906-910. McGraw-Hill, New York, NY.
9. Hulteberg, P. C., J. G. M.Brandin, F. A. Silversand and M. Lundberg (2005) Preferential oxidation of carbon monoxide on mounted and unmounted noble-metal catalysts in hydrogen-rich streams. *International Journal of Hydrogen Energy*, 30(11), 1235-1242.
10. Larentis, A. L., N. S. Resende, V. M. Salim and J. C. Pinto (2001) Modeling and optimization of the combined carbon dioxide reforming and partial oxidation of natural gas. *Appllied Catalysis A*: *General*, 215(1-2), 211-224.
11. Ledjeff-Hey, K., J. Rose and R. Wolters (2000) CO2-scrubbing and methanation as purification system for PEFC. *Journal of Power Sources*, 86(1-2), 556-561.
12. Levent, M. (2001) Water–gas shift reaction over porous catalyst: Temperature and reactant concentration distribution. *International Journal of Hydrogen Energy*, 26(6), 551-558.
13. Pukrushpan, J. T., A. G. Stefanopoulou, S. Varigonda, L. M. Pedersen, S. Ghosh and H. Peng (2003) Control of natural gas catalytic partial oxidation for hydrogen generation in fuel cell applications. Proceeding of the American Control Conference, Denver, Colorado.
14. Pukrushpan, J. T., A. G. Stefanopoulou, S. Varigonda, L. M. Pedersen, S. Ghosh and H. Peng (2005) Control of natural gas catalytic partial oxidation for hydrogen generation in fuel cell applications. *IEEE Transactions on Control System Technology*, 13(1), 3-14.
15. Pukrushpan, J., A. Stefanopoulou, S. Varigonda, J. Eborn and C. Haugsteretter (2006) Control-oriented model of fuel processor for hydrogen generation in fuel cell applications. *Control Engineering Practice*, 14(3), 277-293.
16. Recupero, V., L. Pino, R. D. Leonardo, M. Laganà and G. Maggio (1998) Hydrogen generator, via catalytic partial oxidation of methane for fuel cells. *Journal of Power Sources*, 71(1-2), 208-214.
17. Recupero, V., L. Pino, A. Vita, F. Cipitì, M. Cordaro and M. Laganà (2005) Development of a LPG fuel processor for PEFC systems: Laboratory scale evaluation of autothermal reforming and preferential oxidation subunits. *International Journal of Hydrogen Energy*, 30(9), 963-971.
18. Stein, G. and M. Athan (1987) The LQG/LTR procedure for multivariable feedback control design. *IEEE Transaction on Automatic Control*, AC-32(2), 105-114.
19. Sun, J., J. DesJardins, J. Buglass and K. Liu (2005) Noble metal water gas shift catalysis: Kinetics study and reactor design. *International Journal of Hydrogen Energy*, 30(11), 1259-1264.
20. Tsai, H. L. and C. H. Wang (2006) Optimal temperature control for hydrogen reformer by generalized linear quadratic gaussian / loop transfer recovery method. Proceedings of 2006 CACS Automatic Control Conference, Tamsui, Taiwan.
21. Tsai, H. L. and C. H. Wang (2007) Optimal temperature control for hydrogen reformer by generalized linear quadratic gaussian / loop transfer recovery method. *International Journal of Electrical Engineering*. (Accepted)
22. Tsai, H. L. and J. M. Lin (2005) Non-minimum phase system design by structured uncertainty description and modified performance index in LQG/LTR method. 2005 CACS Automatic Control Conference, Tainan, Taiwan.
23. Tsai, H. L., T. Chiang and C. H. Lin (2004) Structure uncertainty description of non-minimum phase systems in LQG/LTR procedure. 2004 Automatic Control Conference, Chang-Hwa, Taiwan.
24. Tsai, H. L. and C. H. Wang (2006) Optimal temperature control for hydrogen reformer by generalized linear quadratic gaussian / loop transfer recovery method. Proceedings of 2006 CACS Automatic Control Conference, Tamsui, Taiwan.
25. Tsai, H. L. and C. H. Wang (2007) Optimal temperature control for hydrogen reformer by generalized linear quadratic gaussian / loop transfer recovery method. *International Journal of Electrical Engineering*. (Accepted)
26. Zhu, J., D. Zhang and K. D. King (2001) Reforming of CH_4 by partial oxidation: Thermodynamic and kinetic analysis. *Fuel*, 8(7), 899-905.

Received: Jan. 26, 2007 Revised: Mar. 26, 2007
Accepted: May 22, 2007